JGR Atmospheres

RESEARCH ARTICLE
10.1029/2024JD042348

Aerosol Radiation Effect Outweighs VOCs Reactivity Effect on Vertical Ozone Photochemical Features

Zhuyi Jiang[1], Bin Zhu[1], Shuangshuang Shi[2], Siqi Yang[3], Guiqian Tang[4], Wen Lu[5], Junlin An[1], Chunsong Lu[6], Ke Li[7], and Hong Liao[7]

[1]Collaborative Innovation Center on Forecast and Evaluation of Meteorological Disasters and Key Laboratory of Meteorological Disaster, Ministry of Education (KLME), Nanjing University of Information Science & Technology, Nanjing, China, [2]Key Laboratory of Ecosystem Carbon Source and Sink, China Meteorological Administration, Wuxi University, Wuxi, China, [3]Heyuan Meteorological Bureau, Heyuan, China, [4]State Key Laboratory of Atmospheric Environment and Extreme Meteorology, Institute of Atmospheric Physics, Chinese Academy of Sciences, Beijing, China, [5]Hubei Meteorological Service Center, Wuhan, China, [6]Key Laboratory for Aerosol-Cloud-Precipitation of China Meteorological Administration, Collaborative Innovation Centre on Forecast and Evaluation of Meteorological Disasters (CIC-FEMD), Nanjing University of Information Science & Technology, Nanjing, China, [7]Joint International Research Laboratory of Climate and Environment Change (ILCEC), Jiangsu Key Laboratory of Atmospheric Environment Monitoring and Pollution Control, Collaborative Innovation Center of Atmospheric Environment and Equipment Technology, School of Environmental Science and Engineering, Nanjing University of Information Science & Technology, Nanjing, China

Key Points:

- Quantifies the impact of aerosol radiation effect (ARE) and VOCs reactivity effect (VRE) on vertical ozone photochemistry
- ARE outweighs VRE on vertical ozone photochemical reactions
- The lower concentrations of precursors (especially NO_2) at high altitudes make the effect of ARE on O_3-NOx-VOC sensitivity more significant

Supporting Information:

Supporting Information may be found in the online version of this article.

Correspondence to:

B. Zhu,
binzhu@nuist.edu.cn

Citation:

Jiang, Z., Zhu, B., Shi, S., Yang, S., Tang, G., Lu, W., et al. (2025). Aerosol radiation effect outweighs VOCs reactivity effect on vertical ozone photochemical features. *Journal of Geophysical Research: Atmospheres*, *130*, e2024JD042348. https://doi.org/10.1029/2024JD042348

Received 27 AUG 2024
Accepted 27 APR 2025

Author Contributions:

Conceptualization: Zhuyi Jiang
Data curation: Siqi Yang
Funding acquisition: Bin Zhu, Shuangshuang Shi
Methodology: Bin Zhu, Junlin An
Resources: Bin Zhu, Guiqian Tang
Software: Shuangshuang Shi, Wen Lu
Supervision: Siqi Yang
Validation: Zhuyi Jiang
Visualization: Zhuyi Jiang
Writing – original draft: Zhuyi Jiang
Writing – review & editing: Bin Zhu, Chunsong Lu, Ke Li, Hong Liao

Abstract The proportion of more active volatile organic compounds (VOCs) species decreases with altitude, whereas radiation increases vertically due to aerosol scattering near the surface, exerting opposite effects on vertical O_3 generation. Using the observation-based model (OBM) constrained by vertical profiles, we identified that the aerosol radiation effect (ARE) has a stronger impact on photochemical characteristics and O_3-NOx-VOC sensitivity than the VOCs reactivity effect (VRE). ARE is the dominant factor, promoting the formation of O_3 and ·OH (increases by 36.7% and 106.3%), enhancing high-altitude oxidation, and shifting parts of the VOC-limited regimes to the NOx-limited regimes (VOCs/NOx ratio decreases by 21.1%). Additionally, rapid NOx depletion with altitude leads to stronger NOx limitation aloft, amplifying ARE's effect on O_3-NOx-VOC sensitivity (ratio decreases by 28.1%). These findings improve the understanding of vertical ozone generation conditions and suggest that more attention should be paid to vertical environments in surface ozone management.

Plain Language Summary Ozone is formed by the photochemical reaction of volatile organic compounds (VOCs) and nitrogen oxides (NOx) under solar radiation. Some aerosol particles near the surface can scatter sunlight, enhancing the vertical aerosol radiation effect (ARE) on the above air, which accelerates the reactions that produce ozone therein. Conversely, active VOCs decrease with increasing altitude (VOCs reactivity effect, VRE), resulting in reduced ozone generation. This study found that ARE has a greater impact on vertical ozone photochemical characteristics and O_3-NOx-VOC sensitivity than VRE. ARE drives ozone and ·OH production, enhancing atmospheric oxidation at high altitudes and making the upper atmosphere more NOx-limited. Additionally, the concentration of high-altitude precursors is severely attenuated (especially NO_2), making the effect of ARE on O_3-NOx-VOC sensitivity more significant. Recognizing these effects could increase awareness of vertical ozone pollution and aid in improving air quality management and ozone pollution control.

1. Introduction

Tropospheric ozone, a typical secondary pollutant, is generated through complex, nonlinear interactions influenced by various environmental conditions such as solar radiation, temperature, and the concentrations and reactivity of precursors such as nitrogen oxides (NOx) and volatile organic compounds (VOCs), along with their ratios (Lin et al., 1988; Liu et al., 2020). Understanding the vertical photochemistry of ozone is not only to deepen our knowledge of the processes governing ozone production and consumption but also sheds light on its broader impacts on climate and near-surface air quality (Bourgeois et al., 2020; Godowitch et al., 2011; He et al., 2022; Wu et al., 2024; Zhang et al., 2021). Efforts to characterize ozone's behavior date back to Dodge (1977), who established the Empirical Kinetics Modeling Approach (EKMA) curves using the Ozone Isopleth Plotting

Package (OZIPP) to describe the relationship between O_3-NOx-VOCs. Cardelino and Chameides (1995) developed an Observation-Based Model (OBM) based on relative incremental reactivity (RIR) to diagnose the relationship between O_3 production, consumption and its precursors under actual atmospheric pollution conditions. Since then, several commonly used OBM mechanisms have emerged, including CBM, RACM, MCM and NCAR-MM. (Guo et al., 2013; Kanaya et al., 2009; Ran et al., 2012; Song et al., 2022).

Many studies on O_3-NOx-VOC sensitivity have indicated that metropolitan areas are often VOC-limited regimes, whereas a small number of urban and rural areas are primarily NOx-limited or VOC-NOx co-limited regimes. (Liu et al., 2021, 2023; Sillman et al., 1990; Tan et al., 2018; Wang et al., 2023). The reduction in radiation significantly decreases O_3 production efficiency (Deng et al., 2011), correspondingly increasing the ridge line of the EKMA curve (VOCs/NOx ratio) (An et al., 2021) causing some regions that were previously NOx-limited to transition to VOC-limited regimes. Radiation also induces the photolysis of O_3 to produce hydroxyl radicals (·OH), which are crucial for the atmospheric oxidation efficiency (Levy, 1972; Thompson, 1992). Additionally, due to significant differences in the chemical reactivity of VOCs, their contributions to O_3 formation vary greatly (Atkinson, 2000). Generally, alkenes and aromatics are the major contributors to ozone formation potential (OFP) (Hui et al., 2020; Yadav et al., 2024; Zhang et al., 2023). Numerous observations have shown that the more photochemically active VOCs species tend to decreases with increasing altitude, meaning the proportion of reactive species decreases with altitude (Sun et al., 2018; Wu et al., 2020, 2021). When the proportion of chemically active species is low, the efficiency of providing $\cdot HO_2$ and $\cdot RO_2$ decreases, which increases the ridge of the EKMA curve (VOCs/NOx ratio) (Zhu et al., 2006).

By adjusting the dilution ratios of NOx and VOCs in urban conditions, Dieter (1997) diagnosed the variation of surface photochemical characteristics in the horizontal direction from urban-suburban-remote areas. Observations (Jiang et al., 2018; Li et al., 2019) have shown that the decrease of VOCs and NOx concentrations is much greater vertically than horizontally, implying that just 1–2 km altitude difference could result in species concentrations attenuation and dilution ratios similar to those over hundreds of kilometers horizontally. Moreover, the photochemical environment, such as aerosol, radiation, temperature and humidity, varies significantly in the vertical direction, leading to substantial differences in O_3 generation. Previous OBM studies on O_3 photochemical characteristics and O_3-NOx-VOC sensitivity have predominantly relied on surface-based observations, with less emphasis on the vertical environment. Therefore, an integrated exploration of the vertical O_3-precursors and O_3-radiation relationships holds broader scientific significance.

It is noteworthy that VOCs concentrations and the proportion of more reactive species generally decreases with altitude, inhibiting O_3 formation more than at the surface (VOCs reactivity effect, VRE). Conversely, under most conditions of high aerosol pollution, the photolysis rate increases with altitude due to aerosol scattering (aerosol radiation effect, ARE) (Dickerson et al., 1997; Gao et al., 2020; Shi et al., 2022), thereby promotes O_3 formation. Both effects exert different impacts on photochemical characteristics such as net ozone production rate (PO_3), ·OH concentrations, and $\cdot(RO_2 + HO_2)$ concentrations. In this study, vertical profiles from a fall filed campaign in Nanjing, China, along with an observation-based model (OBM), were used to study the vertical photochemical reaction processes of O_3. We systematically analyzed the impacts of the ARE, VRE, and precursor concentrations attenuation on O_3 photochemical characteristics and O_3-NOx-VOC sensitivity. Our findings aim to offer new insights and theoretical foundations for combating photochemical pollution.

2. Materials and Methods

2.1. Observations and Models

The observation site is situated in the Intelligent Manufacturing Industrial Park in the northern suburbs of Nanjing (32°26′N, 118°72′E), a mixed industrial and rural area with no obvious sources of air pollution emissions within a 1.0 km radius (Figure 1).

This study utilized an unmanned aerial vehicle (UAV) platform equipped with a sampling system (Tedlar sampling air bags and wireless remote-control miniature sampling pumps (Wu et al., 2020)) to collect VOCs samples from the surface to 1 km. Air samples at different altitudes were collected into Tedlar bags using a dedicated sampling pump. To minimize contamination, the bags were pre-cleaned with high-purity nitrogen and shielded from sunlight using black covers. During sampling, the UAV ascended at a steady speed of 2.5 m/s without stopping. Ground-level samples (~2 m) were taken before takeoff, whereas subsequent samples

Figure 1. Observation site and surrounding environment.

represented atmospheric layers within a vertical range of ±100 m (samples collected between 100 and 300 m are represented as air samples at a mean altitude of 200 m). The entire process, including pump operation, was remotely controlled. The pump flow rate was set to 2 L/min, with each sample collected in approximately 1 minute. The sampling period was from 18 October 2020 to 15 November 2020, at 8:00, 14:00, and 20:00 daily (LT). The VOCs laboratory analysis process was consistent with Wu et al. (2020, 2021), using a TH-300B VOCs online monitoring system and gas chromatography-mass spectrometry/flame ionization detector (GC-MS/FID, 2010SE). Samples were transported to the laboratory within 48–72 hr of collection. Analysis involved pre-concentration by the TH-300B system, followed by GC-MS/FID processing. The system utilized two channels: FID and MS. The FID channel condensed and dehydrated samples at −50°C, removed CO_2 with an adsorption tube, and captured C2–C5 hydrocarbons using a PLOT capillary column at −150°C. The MS channel condensed and dehydrated samples at −20°C, using a passivated capillary column to capture C6–C12 hydrocarbons and halogenated hydrocarbons at −150°C. A total of 87 VOCs components were measured, including 28 alkanes, 12 alkenes, 16 aromatics, 30 halogenated hydrocarbons, and acetylene. Detailed components, average concentrations, and detection limits are provided in Table S1 in Supporting Information S1.

The UAV also carried PDR-1500 and AE51 instruments to obtain vertical concentration profiles of $PM_{2.5}$ and black carbon (BC). Simultaneously, another UAV collected profiles of NO_2, O_3, and ultraviolet radiation. Throughout the sampling process, the observation data of these elements can be monitored, stored and transmitted in real time. Meteorological sounding data were captured by GPS meteorological sounding balloons at a resolution of 1 s. The instruments were described in detail in our previous study (Yang et al., 2024). In total, vertical observations yielded 61 effective profiles of VOCs, 65 effective profiles of NO_2, 76 effective profiles of meteorological elements, 83 effective profiles of $PM_{2.5}$, BC, and O_3 concentrations, and 81 effective profiles of radiation.

2.2. Observation-Based Model and Experiment Design

To calculate aerosol optical parameters, daily averages of actual vertical profiles of $PM_{2.5}$ and BC were utilized in conjunction with the Optical Properties of Aerosols and Clouds (OPAC) model (Hess et al., 1998) (Table S1 in Supporting Information S1). The simulated optical parameters were subsequently averaged and used in the Tropospheric Ultraviolet and Visible radiation (TUV) model to obtain the photolysis coefficients required for photochemical reactions (Madronich & Flocke, 1999). Finally, the initial pollutant gas components and their average volume mixing ratios at 8:00 a.m. (including CO, NOx, and VOCs, obtained from vertical observations)

Table 1
Experimental Settings to Identify the Two Effects (Aerosol Radiation Effect and VOCs Reactivity Effect) on Ozone Photochemical Reaction Processes

Experiment name	Range of precursor concentration variations at corresponding altitude (m)	Proportion of VOCs species at corresponding altitude (m)	Radiation intensity at corresponding altitude (m)
1.Exp_p0v0r0[a]	0	0	0
2.Exp_p0v400r0	0	400	0
3.Exp_p0v800r0	0	800	0
4.Exp_p0v800r400	0	800	400
5.Exp_p0v800r800	0	800	800
6.Exp_p0v400r400	0	400	400
7.Exp_p400v400r400	400	400	400
8.Exp_p800v800r800	800	800	800

[a]p0 represents the range of precursor concentration variations at the surface, v0 the VOCs species proportion at the surface, and r0 the radiation at the surface. As such, Exp_p0v0r0 represents the experiment with VOCs species proportion, radiation condition and precursor variation ranges at the surface. Exp_p400v400r400 represents the experiment with all the conditions of precursor variation ranges, VOCs species proportion, and radiation at 400 m.

were employed by the National Center for Atmospheric Research Master Mechanism (NCAR-MM) model to compute the formation of O_3, radicals, and intermediates. Due to limitations in observational instruments, the vertical concentration profile of NO could not be directly obtained. However, previous studies (Chen et al., 2025; Silvern et al., 2018; Yang et al., 2023) have shown that within the 0–1 km range of the boundary layer, the NO_2/NO concentration ratio remains relatively constant with height under local atmospheric conditions. This stability is attributed to the photostationary-state relationship among NO, NO_2, O_3, and solar radiation. Therefore, in this study, we estimated the vertical profile of NO based on the observed surface-level NO_2/NO ratio (~2) (Figure S1 in Supporting Information S1) and the measured vertical profile of NO_2. This inferred NO profile was then applied in the model simulations.

The model can simulate the temporal evolution of chemical composition within an air mass without horizontal transport. In this study, parameters such as the daily variation in boundary layer height and dilution intensity were not set. It was simply regarded as an idealized reaction environment constrained only by the concentrations of precursors. For more detailed description of these models refers to the study by Shi et al. (2022). This study considered 34 VOCs species, identified by NCAR-MM, that significantly contribute to photochemical reactions, comprising 22 alkanes, 6 alkenes, 5 aromatics, and acetylene (Table S2 in Supporting Information S1). A total of 900 simulation scenarios were generated by varying the VOCs and NOx concentrations (with concentration adjustment factors ranging from 0.1 to 3.0 at intervals of 0.1), and the maximum ozone concentration of each simulation result was selected to construct the O_3 isoline curve, referred to as origin-EKMA.

In the NCAR-MM model, the total generation rate (G_{O_3}), consumption rate (D_{O_3}) and net generation rate (P_{O_3}) of O_3 can be expressed as Equations 1–3:

$$G_{O_3} = k_{HO_2+NO}[HO_2][NO] + \sum k_{RO_2+NO}[RO_2][NO] \quad (1)$$

$$D_{O_3} = k_{HO_2+O_3}[HO_2][O_3] + k_{OH+O_3}[OH][O_3] + k_{O(1D)+H_2O}[O(1D)][H_2O] + k_{OH+NO_2}[OH][NO_2] + k_{alkenes+O_3}[alkenes][O_3] \quad (2)$$

$$P_{O_3} = G_{O_3} - D_{O_3} \quad (3)$$

In the formula, k represents the reaction rate constant for each reaction.

2.3. Experimental Settings

Building upon the origin-EKMA, sensitivity experiments were conducted by varying the proportion of reactive VOCs species, aerosol radiation intensity, and the range of precursor concentrations, respectively, as shown in Table 1. Experiments 1–6 assume that precursor concentrations at each altitude are consistent with those at the

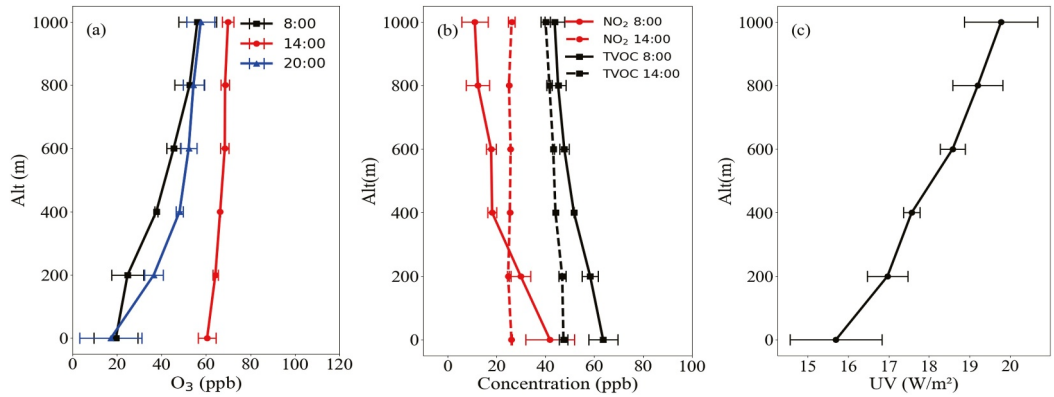

Figure 2. Average vertical profiles of O_3 (a), NO_2, and volatile organic compounds concentrations (b), and UV radiation (c).

surface to examine the impacts of ARE, VRE and the integrated effects of both on the photochemical characteristics and O_3-NOx-VOC sensitivity, excluding interference from variations in precursor concentrations. In the absence of fresh NOx, NOx depletes more rapidly than VOCs, causing the instantaneous VOCs/NO_2 ratio to increase with time, thereby inhabiting production of O_3 (Seinfeld & Pandis, 2006). Vertically, precursor concentrations also attenuate (especially NO_2), leading to an increase in the VOCs/NO_2 ratio with altitude. Therefore, we designed experiments 7 and 8 to further examine the integrated effects of ARE and VRE across the actual range of precursor concentration
variations at different altitudes.

3. Results

3.1. Vertical Observation Features of O_3, Its Precursors and Ultraviolet Radiation

Figure 2 shows the vertical distribution features of O_3, NO_2, and VOCs concentrations, along with ultraviolet radiation during the observation period. The O_3 concentration is lowest at each altitude at 8:00, which is due to the stagnation of O_3 production and the titration of NO at night. Daytime photochemical processes elevate O_3 concentration to their peak in the afternoon. At the same time, strong turbulence transport makes the vertical distribution of O_3 more uniform. Around 20:00, the titration effect of NO rapidly decreases surface O_3 levels, whereas the upper layer (>400 m) retains higher concentrations due to a weaker titration effect. In Figure 2b, both NO_2 and VOCs concentrations decrease with altitude in the early morning, but NO_2 decreases more sharply than VOCs, causing the VOCs/NO_2 ratio to increase from 1.5 at the surface to 4.0 at 1,000 m. At 14:00, stronger atmospheric turbulence leads to a more uniform distribution of NO_2 and VOCs in the vertical direction, which results in smaller fluctuations (standard deviation) in their concentrations. More importantly, with the increase in altitude, the concentration proportion of more reactive VOCs species decreases significantly (Figure 3). For example, the proportion of species with strong reactivity (alkenes + ARO2) is 12.0% at the surface, 7.7% at 400 m, and 5.5% at 800 m.

Additionally, Figure 2c illustrates that UV radiation increases with altitude, rising by approximately 4 W/m^2 from the surface to 1,000 m. The increase in radiation intensity will increase the photolysis rate of NO_2, thereby promoting the formation of ozone (Zhao, Hu, Du, et al., 2021; Zhao, Hu, Liu, et al., 2021).

3.2. OBM Revealed Vertical O_3 Production and Photochemical Characteristics

Figure 4 displays the EKMA-O_3 and EKMA-$OH_{\_12\ hr}$ curves obtained in Experiments 1–8. From the results of experiments 1-2-3 (Figures 4a–4c), it can be seen that the proportion of reactive species decreases with increasing altitude under the same surface radiation conditions. The maximum ozone ($O_{3,max}$) concentration at the reference points in Figure 4c decreases by nearly 20 ppb from the surface to 800 m, a reduction of 12.3%. The average concentration of ·OH over 12 hr ($OH_{\_12\ hr}$) shows a slight decrease of 8.0%. At this time, the corresponding ridge (VOCs/NOx ratio) of EKMA curve increases from 5.7 at the surface to 6.8 at 800 m, consistent with findings by Zhu et al. (2006). As a result, certain regions originally located in NOx-limited regimes transiting to VOC-limited regimes. Experiments 1-2-3 indicate that the weakening of VOCs reactivity inhibits the photochemical reactions

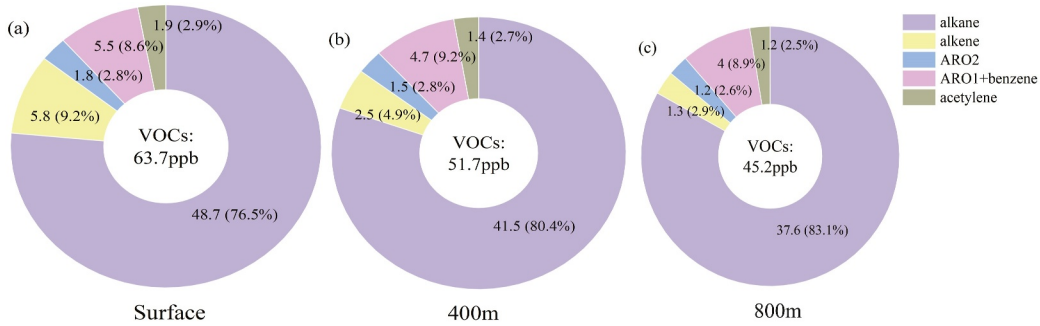

Figure 3. Average proportion of volatile organic compounds (VOCs) concentrations (08:00) at surface (a), 400 m (b), and 800 m (c). This study refers to the SAPRC chemical mechanism (classification based on the reactivity of VOCs components with OH radical) (Carter, 2010). It categorizes benzene and ARO1 as aromatic hydrocarbons with weak reactivity, whereas ARO2 exhibits strong reactivity; for alkenes, all of them are substances with strong reactivity; alkanes and acetylene are inactive species.

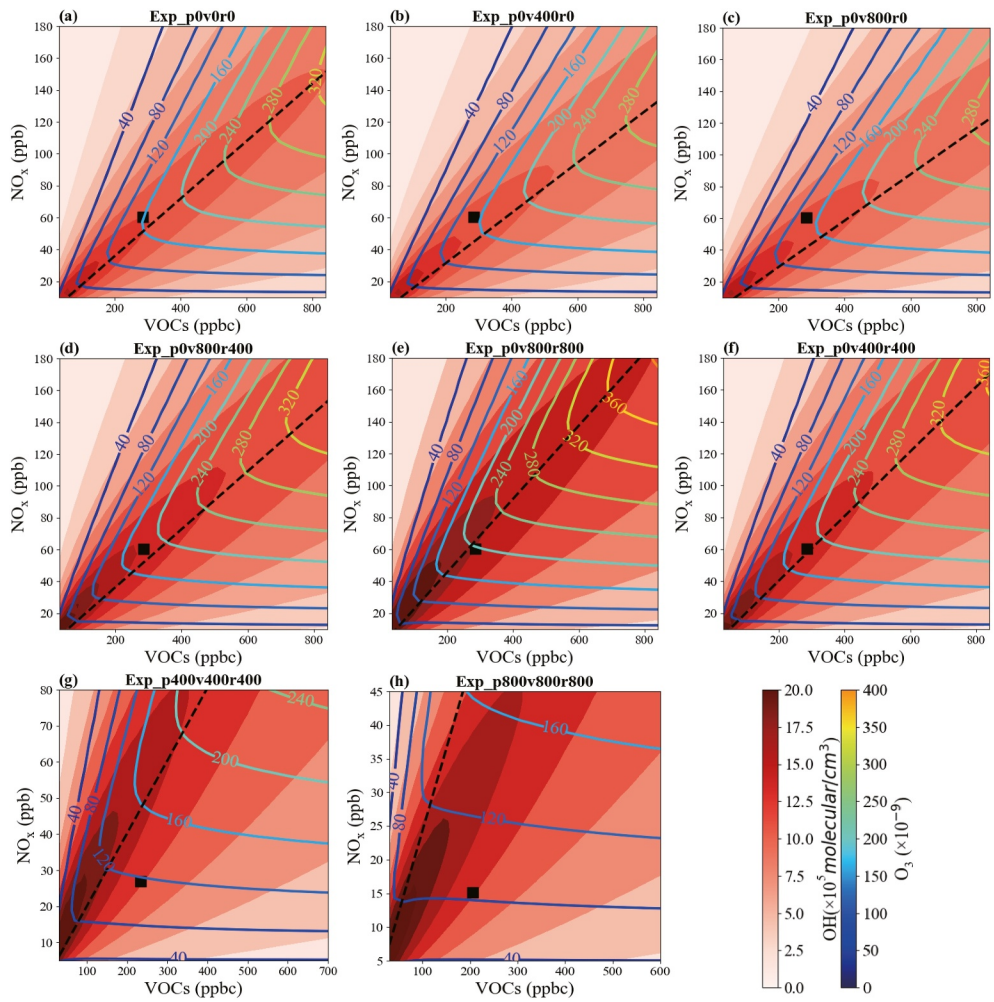

Figure 4. The O_3 daily maximum concentration curve is generated by each group of experiments (the isoline represents the O_3 daily maximum concentration, the black dashed line denotes the ridge of the curve, the color-filled graph represents the 12 hr ·OH average concentration isoline, and the black points indicate the real concentrations of precursors at surface in panels (a–f), and at 400 and 800 m in panels (g and h), respectively, which are called reference points).

Table 2
Photochemical Characteristics at the Reference Point of Each Group of Experiments (PO_3, ·OH and ·(HO_2 + RO_2) Concentrations at the $O_{3,max}$ Concentration)

Experimental name	PO_3 ($\times 10^{-9}$/h)	Concentration of ·OH ($\times 10^5$ molecular/cm^3)	Concentration of ·(HO_2 + RO_2) ($\times 10^8$ molecular/cm^3)	VOCs/NOx ratio at EKMA ridge line
1.Exp_p0v0r0	4.9	6.3	6.4	5.7
2.Exp_p0v400r0	4.4	5.4	5.5	6.4
3.Exp_p0v800r0	3.9	4.8	4.4	6.8
4.Exp_p0v800r400	5.3	8.4	12.7	5.5
5.Exp_p0v800r800	6.6	13.0	22.1	4.5
6.Exp_p0v400r400	5.9	8.6	14.6	4.9
7.Exp_p400v400r400	3.0	8.7	18.0	5.0
8.Exp_p800v800r800	2.1	9.4	22.8	4.1

of O_3,ies slightly weakens the oxidizing capacity of the upper atmosphere, and makes the O_3-NOx-VOC sensitivity more inclined to VOC-limited regimes.

However, when fixing the proportion of reactive VOCs species and solely enhancing aerosol radiation intensity (Experiments 3-4-5 and Figures 4c–4e), $O_{3,\ max}$ increases by nearly 66.9 ppb from the surface to 800 m, marking a 49.3% increase. Similarly, $\cdot OH_{\_12\ hr}$ increases significantly from 1.0×10^6 molecules/cm^3 to 1.7×10^6 molecules/cm^3, an increase of approximately 70.0%, indicating a more oxidizing atmosphere at high altitudes compared to the surface. The EKMA curve ridge (VOCs/NOx ratio) decreases from 6.8 at the surface to 4.5 at 800 m, resulting in a steeper ridge. Parts of the regions originally located in the VOC-limited regimes transiting to NOx-limited regimes, aligning with findings of An et al. (2021). Experiments 3-4-5 demonstrate that intensified radiation promotes the photochemical reactions of O_3, enhances upper atmospheric oxidation, and shifts O_3-NOx-VOC sensitivity to NOx-limited regimes.

Combining both effects (Experiments 1-6-5, Figures 4a, 4f, and 4e) reveals a consistent upward trend in $O_{3,max}$, increasing by approximately 48.6ppb from the surface to 800 m (a 31.6% increase). $\cdot OH_{\_12\ hr}$ also increases with altitude, from about 1.1×10^6 molecules/cm^3 to 1.7×10^6 molecules/cm^3 (a 54.5% increase), indicating heightened atmospheric oxidation at higher altitudes. Furthermore, the EKMA curve ridge (VOCs/NOx ratio) decreases from 5.7 at the surface to 4.5 at 800 m, steepening the ridge and shifting parts of regions initially in VOC-limited regimes to NOx-limited regimes. Experiments 1-5-6 comparing with experiments 1-2-3 and 3-4-5, when keeping a consistent range of precursor concentrations (at the surface), we confirm that ARE predominates over VRE when considering the integrated effects of both radiation and VOCs species reactivity varying with altitude. ARE plays a dominant role in the vertical change of O_3 photochemical reaction processes, enhances upper atmospheric oxidation, and contributes prominently to the transition toward NOx-limited regimes at higher altitudes.

Table 2 presents the quantitative impacts of ARE and VRE, showing the calculated values of each photochemical characteristics at the reference point in Figure 3. Under the influence of VRE (Experiments 1-2-3), $\cdot HO_2$ and $\cdot RO_2$ provision by VOCs decrease, along with the rate of PO_3 and ·OH also decreases by 20.4% and 23.8%, respectively. Conversely, under the influence of ARE (Experiments 3-4-5), enhanced radiation stimulates the reactivity of VOCs species, resulting in a significant increase in ·(HO_2 + RO_2) concentration and a larger PO_3 (a 69.2% increase). Additionally, ·OH concentration rises from 4.8×10^5 molecular/cm^3 at the surface to 1.3×10^6 molecular/cm^3 at 800 m (a 170.8% increase). This aligns with previous studies in the Pearl River Delta (Lu et al., 2012; Yang et al., 2022), where ·OH concentrations were higher in rural areas than urban ones, due to stronger solar radiation in rural regions. When integrating both effects, ·(HO_2 + RO_2) concentration increases, accompanied by a rise in PO_3 from 4.9×10^{-9}/h at the surface to 6.6×10^{-9}/h at 800 m, marking a 34.7% increase. Similarly, the concentration of ·OH rises from 6.3×10^5 to 1.3×10^6 molecular/cm^3, reflecting a 106.3% increase. The results of photochemical characteristics align with EKMA-O_3 findings, highlighting ARE's stronger impact on ozone photochemical processes compared to VRE, which serves as the primary driver of ozone characteristics changes.

In experiments 7 and 8, we further examine the impact of the integrated effects of ARE and VRE on photochemical characteristics and O_3-NOx-VOC sensitivity under the sharp decrease of precursors and high VOCs/NOx ratios within real vertical profile ranges. The results of the experiments 1-7-8 (Figures 4a, 4g, and 4h and

Table 2) reflect that under the combined effect of precursor concentrations attenuation, $O_{3,max}$ decreases significantly, with a reduction of up to 45.3% from the surface to 800 m, and PO_3 also shows a decreasing trend (57.1% decrease). This is mainly due to the reaction conditions being constrained solely by precursor concentrations, under which VOCs and NO_x concentrations decrease significantly with increasing altitude. However, $OH_{\_12\ hr}$ concentration increases from 1.1×10^6 to 1.2×10^6 molecular/cm^3 (9.1% increase) with altitude, and the corresponding ·OH concentration at $O_{3,max}$ increases by 49.2%. This is mainly because ·OH concentration is strongly correlated with radiation intensity (Rohrer & Berresheim, 2006). As such, even if the precursor concentrations drop significantly, ·OH concentration increases instead. The radiation enhancement effect also makes the concentration of $\cdot(HO_2 + RO_2)$ higher. The EKMA curve ridge (VOCs/NOx ratio) decreases from 5.7 at the surface to 4.1 at 800 m, a decrease of 28.1%, which is a larger change than when there is no precursor concentrations attenuation (21.1%). This indicates that the shift of the ridge is more pronounced within the real range of vertical precursor changes, leading to the phenomenon where some regions originally VOC-limited more clearly transiting to NOx-limited regimes.

Compared to experiments 1-6-5, the concentrations of O_3 and PO_3 exhibits a downward trend with the superimposed precursor concentrations attenuation. However, other changes are consistent with the results of Experiments 1-6-5. Therefore, it is concluded that when the concentration of precursors variations, the influence of ARE on the ozone photochemical characteristics and O_3-NOx-VOC sensitivity still outweighs VRE. It is worth noting that precursor's attenuation facilitates the transition to NOx-limited conditions at higher altitudes due to the lack of NOx, thereby making the impact of ARE on O_3-NOx-VOC sensitivity more pronounced.

4. Conclusion

Our vertical observations showed that the concentrations of both VOCs and NO_2 decrease with altitude, but the decrease of NO_2 is more dramatic, causing the VOCs/NOx ratios to significantly increase with altitude. Meanwhile, UV radiation increases with altitude. The proportion of reactive VOCs species is highest at the surface (12.0% in the morning), and lowest at 800 m (5.5%). Combined with OBM simulations, we explored the impacts of vertical ARE, VRE and precursor concentrations attenuation on the O_3 photochemical reaction.

We found that, regardless of precursor concentrations, a decrease in the proportion of reactive VOCs species led to a gentler EKMA ridge (increased VOCs/NOx ratio), whereas an increase in radiation intensity resulted in a steeper EKMA ridge (decreased VOCs/NOx ratio). Furthermore, ARE had a greater impact than VRE on ozone vertical photochemical characteristics and O_3-NOx-VOC sensitivity. Under the influence of the dominant factor ARE, PO_3 increased by 36.7% from the surface to 800 m, whereas OH radical concentrations rose by 106.3%, accelerating O_3 and ·OH formation, enhancing upper-layer oxidation, and stimulating the reactivity of less active VOCs, thereby facilitating $\cdot HO_2$ and $\cdot RO_2$ production (approximately doubled). Simultaneously, increased radiation intensity facilitated the transition from VOC-limited regimes at the surface to NOx-limited regimes at high altitudes. It is worth noting that under actual atmospheric conditions, a decrease in the concentration of precursors (especially NO_2) caused the ridge of the EKMA curve to shift more significantly, with the slope decreasing by 28.1%, which is larger than the change when there is no precursor concentration attenuation (21.1%). This further reinforced the transition of the upper atmosphere to a NOx-limited regimes, thereby amplifying the impact of ARE on O_3-NOx-VOC sensitivity.

It can be expected that these factors may weaken/strengthen VRE under pre-noon (inversion)/afternoon (convection) conditions. However, these factors are unlikely to alter the conclusions of this study. In addition, to assess the potential uncertainty associated with the vertical NO_2/NO concentration ratio on the experimental results of this study, we conducted additional sensitivity experiments using NO_2/NO ratios of 5 and 10. The results indicated that variations in this ratio did not alter our main conclusions. For further details, please refer to the supporting information (Figure S3 and Table S4 in Supporting Information S1). This paper aims to reveal the vertical environments that affect vertical ozone photochemical production, provide new perspectives for ozone pollution management, and suggest that policymakers should pay closer attention to the impact of the vertical environment.

Data Availability Statement

The observational and data are placed in https://doi.org/10.5281/zenodo.14752899. (Jiang et al., 2025). The ozone column concentration data are available from https://acdisc.gesdisc.eosdis.nasa.gov/data/Aura_OMI_Level3/

OMTO3e.003/2020/. (Shi et al., 2022). The OPAC model can be acquired from https://zenodo.org/doi/10.5281/zenodo.13309501. (Jiang et al., 2024a). The NCAR MM model can be acquired from https://zenodo.org/doi/10.5281/zenodo.13309609. (Jiang et al., 2024b).

Acknowledgments
This work was supported by the National Natural Science Foundation of China (42021004, 42275115), the Wuxi University Research Start-up Fund for Introduced Talents, China (2023r036).

References

An, J. L., Lv, H., Xue, M., Zhang, Z. F., Hu, B., Wang, J. X., & Zhu, B. (2021). Analysis of the effect of optical properties of black carbon on ozone in an urban environment at the Yangtze River Delta, China. *Advances in Atmospheric Sciences*, *38*(7), 1153–1164. https://doi.org/10.1007/s00376-021-0367-9

Atkinson, R. (2000). Atmospheric chemistry of VOCs and NOx. *Atmospheric environment*, *34*(12–14), 2063–2101. https://doi.org/10.1016/S1352-2310(99)00460-4

Bourgeois, I., Peischl, J., Thompson, C. R., Aikin, K. C., Campos, T., Clark, H., et al. (2020). Global-scale distribution of ozone in the remote troposphere from the ATom and HIPPO airborne field missions. *Atmospheric Chemistry and Physics*, *20*(17), 10611–10635. https://doi.org/10.5194/acp-20-10611-2020

Cardelino, C. A., & Chameides, W. L. (1995). An observation-based model for analyzing ozone precursor relationships in the urban atmosphere. *Journal of the Air & Waste Management Association*, *45*(3), 161–180. https://doi.org/10.1080/10473289.1995.10467356

Carter, W. P. L. (2010). Development of the SAPRC-07 chemical mechanism. *Atmospheric Environment*, *44*(40), 5324–5335. https://doi.org/10.1016/j.atmosenv.2010.01.026

Chen, L., Song, Z., Yao, N., Xi, H., Li, J., Gao, P., et al. (2025). Photostationary state assumption seriously underestimates NOx emissions near large point sources at 10 to 60 m pixel resolution. *Pest Articles and News Summaries*, *122*(7), e2423915122. https://doi.org/10.1073/pnas.2423915122

Deng, X. J., Zhou, X. J., Wu, D., Tie, X. X., Tan, H. B., Li, F., et al. (2011). Effect of atmospheric aerosol on surface ozone variation over the Pearl River Delta region. *Science China Earth Sciences*, *54*(5), 744–752. https://doi.org/10.1007/s11430-011-4172-7

Dickerson, R. R., Kondragunta, S., Stenchikov, G., Civerolo, K. L., Doddridge, B. G., & Holben, B. N. (1997). The impact of aerosols on solar ultraviolet radiation and photochemical smog. *Science*, *278*(5339), 827–830. https://doi.org/10.1126/science.278.5339.827

Dieter, K. (1997). Tropospheric chemistry and transport. *Science*, *276*(5315), 1043–1044. https://doi.org/10.1126/science.276.5315.1043

Dodge, M. C. (1977). Combined use of modeling techniques and smog chamber data to derive ozone precursor relationships. In B. Dimitriades (Ed.), *Proceedings of the international conference on photochemical oxidant pollution and its control* (Vol. II, pp. 881–889). NC: U.S. EPA.

Gao, J. H., Li, Y., Zhu, B., Hu, B., Wang, L. L., & Bao, F. W. (2020). What have we missed when studying the impact of aerosols on surface ozone via changing photolysis rates? *Atmospheric Chemistry and Physics*, *20*(18), 10831–10844. https://doi.org/10.5194/acp-20-10831-2020

Godowitch, J. M., Gilliam, R. C., & Rao, S. T. (2011). Diagnostic evaluation of ozone production and horizontal transport in a regional photochemical air quality modeling system. *Atmospheric Environment*, *45*(2011), 3977–3987. https://doi.org/10.1016/j.atmosenv.2011.04.062

Guo, H., Ling, Z. H., Cheung, K., Jiang, F., Wang, D. W., Simpson, I. J., et al. (2013). Characterization of photochemical pollution at different elevations in mountainous areas in Hong Kong. *Atmospheric Chemistry and Physics*, *13*(8), 3881–3898. https://doi.org/10.5194/acp-13-3881-2013

He, C., Lu, X., Wang, H. L., Wang, H. C., Li, Y., He, G., et al. (2022). The unexpected high frequency of nocturnal surface ozone enhancement events over China: Characteristics and mechanisms. *Atmospheric Chemistry and Physics*, *22*(23), 15243–15261. https://doi.org/10.5194/acp-22-15243-2022

Hess, M., Koepke, P., & Schult, I. (1998). Optical properties of aerosols and clouds: The software package OPAC. *Bulletin of the American Meteorological Society*, *79*(5), 831–844. https://doi.org/10.1175/1520-0477(1998)079<0831:OPOAAC>2.0.CO;2

Hui, L. R., Liu, X. G., Tan, Q. W., Feng, M., An, J. L., Qu, Y., et al. (2020). VOC characteristics, chemical reactivity and sources in urban Wuhan, central China. *Atmospheric Environment*, *224*, 117340. https://doi.org/10.1016/j.atmosenv.2020.117340

Jiang, M. Q., Lu, K. D., Su, R., Tan, Z. F., Wang, H. L., Li, L., et al. (2018). Ozone formation and key VOCs in typical Chinese city clusters (in Chinese). *Chinese Science Bulletin*, *63*(12), 1130–1141. https://doi.org/10.1360/N972017-01241

Jiang, Z. Y., Zhu, B., Shi, S. S., Yang, S. Q., Tang, G. Q., Lu, W., et al. (2024a). The model----aerosol radiation effect outweighs VOCs reactivity effect on vertical ozone photochemical features [Software]. https://zenodo.org/doi/10.5281/zenodo.13309501

Jiang, Z. Y., Zhu, B., Shi, S. S., Yang, S. Q., Tang, G. Q., Lu, W., et al. (2024b). The model----aerosol radiation effect outweighs VOCs reactivity effect on vertical ozone photochemical features [Software]. https://zenodo.org/doi/10.5281/zenodo.13309609

Jiang, Z. Y., Zhu, B., Shi, S. S., Yang, S. Q., Tang, G. Q., Lu, W., et al. (2025). The dataset, aerosol radiation effect outweighs VOCs reactivity effect on vertical ozone photochemical features [Dataset]. https://doi.org/10.5281/zenodo.14752899

Kanaya, Y., Pochanart, P., Liu, Y., Li, J., Tanimoto, H., Kato, S., et al. (2009). Rates and regimes of photochemical ozone production over central East China in June 2006: A box model analysis using comprehensive measurements of ozone precursors. *Atmospheric Chemistry and Physics*, *9*(20), 7711–7723. https://doi.org/10.5194/acp-9-7711-2009

Levy, H. II. (1972). Photochemistry of the lower troposphere. *Planetary and Space Science*, *20*(6), 919–935. https://doi.org/10.1016/0032-0633(72)90177-8

Li, K., Li, J. L., Tong, S. R., Wang, W. G., Huang, R. J., & Ge, M. F. (2019). Characteristics of wintertime VOCs in suburban and urban Beijing: Concentrations, emission ratios, and festival effects. *Atmospheric Chemistry and Physics*, *19*(12), 8021–8036. https://doi.org/10.5194/acp-19-8021-2019

Lin, X., Trainer, M., & Liu, S. C. (1988). On the nonlinearity of the tropospheric ozone production. *Journal of Geophysical Research*, *93*(D12), 15879–15888. https://doi.org/10.1029/JD093iD12p15879

Liu, P. F., Song, H. Q., Wang, T. H., Wang, F., Li, X. Y., Miao, C. H., & Zhao, H. (2020). Effects of meteorological conditions and anthropogenic precursors on ground-level ozone concentrations in Chinese cities. *Environmental Pollution*, *262*, 114366. https://doi.org/10.1016/j.envpol.2020.114366

Liu, Y. X., Geng, G. N., Cheng, J., Liu, Y., Xiao, Q. Y., Liu, L. K., et al. (2023). Drivers of increasing ozone during the two phases of clean air actions in China 2013–2020. *Environmental Science & Technology*, *57*(24), 8954–8964. https://doi.org/10.1021/acs.est.3c00054

Liu, Z. Z., Doherty, R. M., Wild, O., Hollaway, M., & O'Connor, F. M. (2021). Contrasting chemical environments in summertime for atmospheric ozone across major Chinese industrial regions: The effectiveness of emission control strategies. *Atmospheric Chemistry and Physics*, *21*(13), 10689–10706. https://doi.org/10.5194/acp-21-10689-2021

Lu, K. D., Rohrer, F., Holland, F., Fuchs, H., Bohn, B., Brauers, T., et al. (2012). Observation and modelling of OH and HO2 concentrations in the Pearl River Delta 2006: A missing OH source in a VOC rich atmosphere. *Atmospheric Chemistry and Physics*, *12*(3), 1541–1569. https://doi.org/10.5194/acp-12-1541-2012

Madronich, S., & Flocke, S. J. (1999). The role of solar radiation in atmospheric chemistry. In P. Boule (Ed.), *Environmental photochemistry* (pp. 14–15). Springer. https://doi.org/10.1007/978-3-540-69044-3_1

Ran, L., Zhao, C., Xu, W., Han, M., Lu, X., Han, S., et al. (2012). Ozone production in summer in the megacities of Tianjin and Shanghai, China: A comparative study. *Atmospheric Chemistry and Physics*, *12*(16), 7531–7542. https://doi.org/10.5194/acp-12-7531-2012

Rohrer, F., & Berresheim, H. (2006). Strong correlation between levels of tropospheric hydroxyl radicals and solar ultraviolet radiation. *Nature*, *442*(7099), 184–187. https://doi.org/10.1038/nature04924

Seinfeld, J. H., & Pandis, S. N. (2006). Chemistry of the troposphere. In *Atmospheric chemistry and physics: From air pollution to climate change* (2nd ed., pp. 235–236). John Wiley & Sons, Inc.

Shi, S. S., Zhu, B., Tang, G. Q., Liu, C., An, J. L., Liu, D. Y., et al. (2022). Observational evidence of aerosol radiation modifying photochemical ozone profiles in the lower troposphere. *Geophysical Research Letters*, *49*(15), e2022GL099274. https://doi.org/10.1029/2022GL099274

Sillman, S., Logan, J. A., & Wofsy, S. C. (1990). The sensitivity of ozone to nitrogen oxides and hydrocarbons in regional ozone episodes. *Journal of Geophysical Research*, *95*(D2), 1837–1851. https://doi.org/10.1029/JD095iD02p01837

Silvern, R. F., Jacob, D. J., Travis, K. R., Sherwen, T., Evans, M. J., Cohen, R. C., et al. (2018). Observed NO/NO_2 ratios in the upper troposphere imply errors in NO-NO_2-O_3 cycling kinetics or an unaccounted NOx reservoir. *Geophysical Research Letters*, *45*(9), 4466–4474. https://doi.org/10.1029/2018GL077728

Song, K. X., Liu, R., Wang, Y., Liu, T., Wei, L. Y., Wu, Y. X., et al. (2022). Observation-based analysis of ozone production sensitivity for two persistent ozone episodes in Guangdong, China. *Atmospheric Chemistry and Physics*, *22*(12), 8403–8416. https://doi.org/10.5194/acp-22-8403-2022

Sun, J., Wang, Y. S., Wu, F. K., Tang, G. Q., Wang, L. L., Wang, Y. H., & Yang, Y. (2018). Vertical characteristics of VOCs in the lower troposphere over the North China Plain during pollution periods. *Environmental Pollution*, *236*, 907–915. https://doi.org/10.1016/j.envpol.2017.10.051

Tan, Z. F., Lu, K. D., Jiang, M. Q., Su, R., Dong, H. B., Zen, L. M., et al. (2018). Exploring ozone pollution in Chengdu, southwestern China: A case study from radical chemistry to O3-VOC-NOx sensitivity. *Science of the Total Environment*, *636*, 775–786. https://doi.org/10.1016/j.scitotenv.2018.04.286

Thompson, A. M. (1992). The oxidizing capacity of the Earth's atmosphere: Probable past and future changes. *Science*, *256*(5060), 1157–1165. https://doi.org/10.1126/science.256.5060.1157

Wang, D. C., Zhou, J. B., Han, L., Tian, W. N., Wang, C. H., Li, Y. J., & Chen, J. (2023). Source apportionment of VOCs and ozone formation potential and transport in Chengdu, China. *Atmospheric Pollution Research*, *14*(5), 101730. https://doi.org/10.1016/j.apr.2023.101730

Wu, S., Tang, G. Q., Wang, Y. H., Mai, R., Yao, D., Kang, Y., et al. (2021). Vertical evolution of boundary layer volatile organic compounds in summer over the North China plain and the differences with winter. *Advances in Atmospheric Sciences*, *38*(7), 1165–1176. https://doi.org/10.1007/s00376-020-0254-9

Wu, S., Tang, G. Q., Wang, Y. H., Yang, Y., Yao, D., Zhao, W., et al. (2020). Vertically decreased VOC concentration and reactivity in the planetary boundary layer in winter over the North China Plain. *Atmospheric Research*, *240*, 104930. https://doi.org/10.1016/j.atmosres.2020.104930

Wu, W. Q., Ge, Y. Z., Wang, Y., Su, J., Wang, X., Zhou, B., & Chen, J. (2024). Vertical ozone formation mechanisms resulting from increased oxidation on the mountainside of Mount Tai, China. *PNAS Nexus*, *3*(9), 347–358. https://doi.org/10.1093/pnasnexus/pgae347

Yadav, P., Lal, S., Tripathi, S. N., Jain, V., & Mandal, T. K. (2024). Role of sources of NMVOCs in O3, OH reactivity, and secondary organic aerosol formation over Delhi. *Atmospheric Pollution Research*, *15*(5), 102082. https://doi.org/10.1016/j.apr.2024.102082

Yang, L. H., Daniel, J. J., Nadia, K. C., Zhai, S., Bates, K. H., Shah, V., et al. (2023). Tropospheric NO_2 vertical profiles over South Korea and their relation to oxidant chemistry: Implications for geostationary satellite retrievals and the observation of NO_2 diurnal variation from space. *Atmospheric Chemistry and Physics*, *23*(4), 2465–2481. https://doi.org/10.5194/acp-23-2465-2023

Yang, S. Q., Zhu, B., Shi, S. S., Jiang, Z. Y., Hou, X. W., An, J. L., & Xia, L. (2024). Vertical features of volatile organic compounds and their potential photochemical reactivities in boundary layer revealed by in-situ observations and satellite retrieval. *Remote Sensing*, *16*(8), 1403. https://doi.org/10.3390/rs16081403

Yang, X. P., Lu, K. D., Ma, X. F., Gao, Y., Tan, Z. F., Wang, H. C., et al. (2022). Radical chemistry in the Pearl River Delta: Observations and modeling of OH and HO2 radicals in Shenzhen in 2018. *Atmospheric Chemistry and Physics*, *22*(18), 12525–12542. https://doi.org/10.5194/acp-22-12525-2022

Zhang, W., Zou, Y., Zheng, X. D., Wang, N., Yan, H., Chen, Y., et al. (2021). Characteristics of the vertical distribution of tropospheric ozone in late autumn at Yangjiang station in Pearl River Delta (PRD), China. PartI: Observed event. *Atmospheric Environment*, *244*(2021), 117898. https://doi.org/10.1016/j.atmosenv.2020.117898

Zhang, Z. J., Sun, Y. L., & Li, J. (2023). Characteristics and sources of VOCs in a coastal city in eastern China and the implications in secondary organic aerosol and O3 formation. *Science of The Total Environment*, *887*, 164117. https://doi.org/10.1016/j.scitotenv.2023.164117

Zhao, S. M., Hu, B., Du, C. J., Liu, H., Li, M., Liu, J., et al. (2021). Photolysis rate in the Beijing-Tianjin-Hebei region: Reconstruction and long-term trend. *Atmospheric Research*, *256*, 105568. https://doi.org/10.1016/j.atmosres.2021.105568

Zhao, S. M., Hu, B., Liu, H., Du, C., Xia, X., & Wang, Y. (2021). The influence of aerosols on the NO2 photolysis rate in a suburban site in North China. *Science of The Total Environment*, *767*, 144788. https://doi.org/10.1016/j.scitotenv.2020.144788

Zhu, B., An, J. L., Wang, Z. F., & Li, Y. (2006). Relations of diurnal variations of photochemical ozone to its precursors (in Chinese). *Trans Atmos Sci.*, *29*(6), 744–749. https://doi.org/10.13878/j.cnki.dqkxxb.2006.06.003